Journal of Catalysis **189,** 170–183 (2000)
Article ID jcat.1999.2692, available online at http://www.idealibrary.com on IDEAL®

Mechanism of WO_3 Reduction and Carburization in CH_4/H_2 Mixtures Leading to Bulk Tungsten Carbide Powder Catalysts

A. Löfberg,*,[1] A. Frennet,*,[2] G. Leclercq,† L. Leclercq,† and J. M. Giraudon†

*Catalyse Hétérogène CP243, Université Libre de Bruxelles, 1050 Bruxelles, Belgium; and †Laboratoire de Catalyse de Lille, UPRESA CNRS 8010, Université de Lille 1, 59655 Villeneuve d'Ascq Cedex, France

Received June 28, 1999; revised September 9, 1999; accepted September 13, 1999

The mechanism of bulk tungsten carbide catalysts synthesis from WO_3 in CH_4/H_2 mixtures has been studied using temperature programmed reactions associated with CH_4/D_2 exchange reaction and *in situ* X ray diffraction. Various experimental parameters have been studied such as partial pressures of reactants, heating rate, mass of precursor, or flow rate in order to determine the most important steps occurring during the transformation of WO_3 to WC. It is shown that at temperatures below 900–923 K the diffusion within the solid particles is slow with respect to the rate of reduction of the surface, allowing the carburization of the surface in the presence of a core still partially oxidized. At higher temperatures, the diffusion is rapid, leading to a uniform reduction within the solid. In this case the surface is continuously replenished in oxygen thus inhibiting the activation of methane and allowing the carburization to proceed only when the solid is deeply reduced. An inhibiting effect of hydrogen pressure on the interaction of methane with the surface has also been evidenced, an effect which excludes the possibility of an independent control of the reduction process from that of carburization. Finally the role of space velocity has also been elucidated.

Key Words: **tungsten carbide; preparation; carburization; mechanism.**

INTRODUCTION

Carbides and nitrides of transition metals, and in particular of tungsten and molybdenum, have shown to have catalytic properties in a wide range of reactions (1–11). Initially these materials were thought to be potential substitutes of the platinum group metals following the pioneering work of Levy and Boudart (12).

Recently the first practical application of these materials in catalysis has been proposed in the field of space communication technology (13).

[1] To whom correspondence should be addressed. Laboratoire de Catalyse de Lille, UPRESA CNRS 8010, Université de Lille 1, 59655 Villeneuve d'Ascq Cedex, France. Fax: +33 3.20.43.65.61. E-mail: axel.lofberg@univ-lille1.fr.

[2] Senior Research Associate, Belgian FNRS.

The synthesis of such materials has been the subject of only very few publications even though the bulk nature of such binary compounds is essential in the determination of their surface properties. Most synthesis methods are based on temperature programmed reduction and carburization (for carbides) of an oxide precursor and are inspired by that used by Boudart and his coworkers (14–18). This method leads to relatively low surface area samples (a few tens of m^2/g) of rather well defined catalysts which are to be preferred to bulk samples of higher surface area as these will develop a highly microporous texture (19). In order to determine the intrinsic properties of such materials, our approach is to synthesize well-controlled materials, even at the expense of surface area in order to avoid diffusion problems due to a microporous structure and interference of supplementary elements such as a support.

In a previous paper (20) we showed the complexity of the simultaneous reduction and carburization of tungsten oxide by methane–hydrogen mixtures. Comparing to the behavior of tungsten metal, it has been suggested that the mechanism of carburization is a complex competition between reduction of the oxide at the surface of the particles, metal diffusion in the bulk, and surface interaction of the gas phase reactants with the solid. Furthermore it has been shown that according to the final temperature of reaction it is possible to prepare either W_2C or WC.

In this paper, we propose to investigate more deeply the parameters that will influence the delicate balance between bulk and surface phenomena and thus determine which is, or are, the most determining steps in the carburization process.

Temperature programmed reactions have been performed by varying key parameters such as the rate of temperature increase, the pressure of reactants (either H_2 or CH_4 or both), or the mass of precursor. For some experiments, deuterium has been used instead of hydrogen in order to show the interaction between methane and the surface through exchange reaction.

Finally, temperature programmed reactions with simultaneous X-ray diffraction measurements have also been performed.

0021-9517/00 $35.00

EXPERIMENTAL

Temperature programmed reactions were performed in a flow microreactor at total atmospheric pressure (21). The reactor tube (2 cm long, 8 mm internal diameter), was designed and checked to behave as a well mixed reactor. In this way, the composition of the catalysts calculated by mass balance of the gas phase is representative of the composition of the entire sample. Between 25 and 300 mg of WO_3 (Fluka) were placed in a quartz reactor and treated with flowing mixtures of H_2 (99.9995% from BOC or premixed 10% H_2 in Ar Certified Standard from UCAR) and CH_4 (99.9995% from UCAR or premixed 10% CH_4 in Ar Certified Standard from UCAR) diluted in argon (99.9990% from UCAR). Total flow rates typically ranged from 32 to 50 cm^3/min and individual flow rates were adjusted using (Sho-Rate 1355 from Brooks) flowmeters fitted with needle valves (NRS1 from Brooks). The flowmeters were calibrated and regularly checked with soap bubble flowmeters. An Eurotherm 818 regulator was used for the temperature programming of the oven while an 808 Eurotherm indicator measured the temperature of the reactor. The gas phase composition at the outlet of the reactor was measured using a quadrupole mass spectrometer (QMG-420-5 from Balzers) fitted with a two-stage continuous pressure reduction system (GEV-010 from Balzers). This device results in a linear response of the mass spectrometer signal to partial pressure variations in the flow at atmospheric pressure. Through an accurate calibration, the analytical device thus makes it possible to follow the partial pressures of several compounds during the test and to make mass balance calculations of the consumption of reactants and the evolution of products and, by integration, also to calculate the overall composition of the solid in the reactor according to time.

TABLE 1

Summary Table of TPR Experimental Conditions ($P_R = P_{H_2} + P_{CH_4}$)

	Q_{WO_3} (mg)	Flow (cc/min)	P_{H_2} (Torr)	P_{CH_4} (Torr)	β (K/min)	P_R (%)
Carb-A	107.2	50.0	61	14	3	10
Carb-B	94.3	50.5	215	50.5	3	35
Carb-C	96.2	46.5	561	123	3	90
Carb-D	98	46.6	228	53	1	35
Carb-E	97.6	47.5	225	53	6	35
Carb-F	96	49.6	215	55	12	35
Carb-J	25.2	50.1	210	49	3	35
Carb-K	266	50.5	225	53	3	35
Carb-L	135	32.8	180	55	3	35
Carb-M	290	48.3	559	120	3	90

Deuterium (D_2 99.8% isotop. from UCAR) was used for measuring simultaneous exchange with methane during the carburization. In this case the mass spectrometer signal could not be related directly to molecular species in the gas phase due to interference of products on the same m/e ratios (in particular D_2O and CD_4 at $m/e = 20$). Furthermore, in order to avoid the supplementary interference of Ar^{2+} ($m/e = 20$), helium was used as carrier gas instead of argon (He 99.9990% from UCAR). Although the system could not be resolved quantitatively, qualitative results could be obtained by comparing experiments performed with D_2 with those made in the same conditions with H_2.

The bulk structure of the materials was determined by X-ray diffraction in a diffractometer (Siemens D5000) equipped with a high temperature HTK 10 Anton Paar *in-situ* X-ray diffraction cell. Gas mixtures composed of H_2, CH_4, and Ar (total flow rate, 170 cm^3/min; purities, see

TABLE 2

Main TPR Results

	Range, first peak (K)	O_{R1} (O/W)	Range, second peak (K)	O_{R2} (O/W)	T_i (K)	O_i (O/W)	T_c (K)	O_c (O/W)
Carb-A	880 (982) 1041	0.93	1041 (1159) 1223	2.07	1046	2.02	1136	1.01
Carb-B	796 (909) 941	1.12	941 (1021) 1073	1.88	931	1.82	1027	0.80
Carb-C	776 (867) 899	1.40	899 (969) 1007	1.60	830	2.80	830	2.80
Carb-D	766 (844) 876	1.17	876 (958) 1002	1.83	830	2.83	901	2.68
Carb-E	841 (964) 1000	0.96	1000 (1099) 1157	1.94	1005	2.03	1106	0.73
Carb-F	899 (1050) 1083	1.00	1083 (1194) 1223	2.05	1045	2.38	1174	0.91
Carb-J	785 (876) 922	1.59	922 (966) 1010	1.41	890	1.95	898	1.75
Carb-K	776 (918) 962	1.07	962 (1099) 1150_i	1.93	997	1.80	1088	0.75
Carb-L	802 (919) 960	0.98	960 (1072) 1123_i	2.02	931	2.05	1060	1.06
Carb-M	760 (885) 914	1.07	914 (1020) 1063	1.92	890	2.10	1029	0.45

Note. Temperature range of the first reduction peak (maximum in parentheses); O_{R1}, amount of O removed during the first reduction peak relative to W; temperature range of the second reduction peak (maximum in parenthesis); O_{R2}, amount of O removed during the second reduction peak relatively to W; T_i, temperature at which CH_4 starts to react with the solid; O_i, O to W stoichiometry of the solid at T_i; T_c, temperature at which carbon begins to be retained by the solid; O_c, to W stoichiometry of the solid at T_c.

above) was passed through the platinum cell while the XRD patterns were collected. Temperature was increased linearly at 1 K/min but had to be interrupted for about 10 min for the diffraction measurements.

RESULTS

Temperature Programmed Reactions: CH_4–H_2

Table 1 lists the experimental conditions of the TPR experiments in CH_4–H_2 mixtures. Table 2 contains important results such as the range and maximum of temperature of the first and second reduction peaks and the amount of oxygen extracted from the solid relative to W. The temperature and the residual oxygen O/W stoichiometry of the solid at the moment CH_4 starts being consumed are also indicated as well as the equivalent data relative to carbon retention by the solid (carburization by CH_4).

Reactant pressure effect. To illustrate typical results obtained during these experiments only three TPR (Figs. 1 to 3) profiles are shown and this to avoid overloading the paper.

Carb-A, B, and C (Figs. 1 to 3) experiments correspond to a variation of partial pressures of the reactants ($P_R = P_{CH_4} + P_{H_2}$) from 10 to 90% of atmospheric pressure while keeping the ratio of CH_4 to H_2 constant ($CH_4/H_2 = 1/4$) as well as all other parameters.

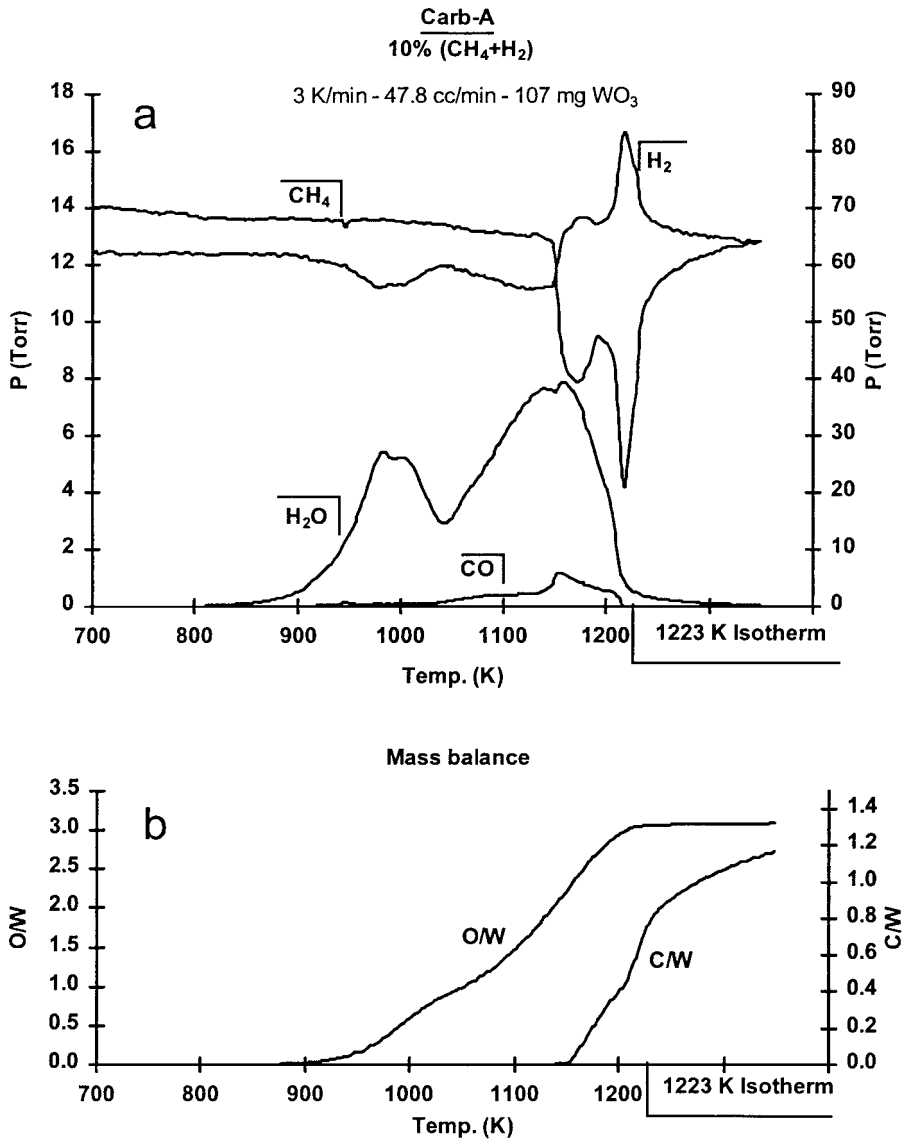

FIG. 1. Carb-A, temperature programmed reaction of WO_3 with $P_R = 10\%$, $P_{CH_4}/P_{H_2} = 1/4$, $\beta = 3$ K/min, $Q_{WO_3} = 107$ mg, $F = 47.8$ cc/min. (a) Partial pressure evolution of CH_4, H_2, H_2O, and CO according to temperature. (b) Mass balance calculation according to temperature of the amount of oxygen removed from the solid relative to tungsten (O/W) and of carbon retained by the solid (C/W).

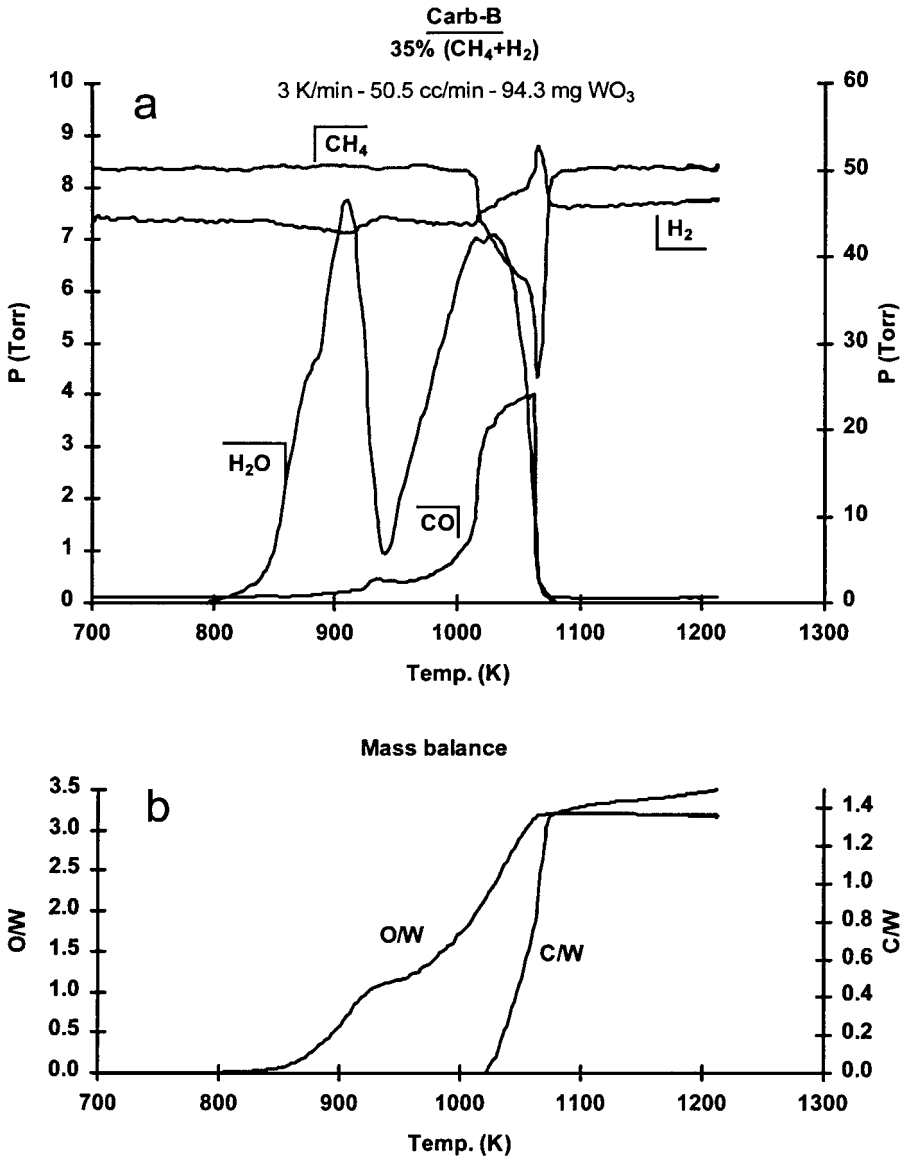

FIG. 2. Carb-B, temperature programmed reaction of WO_3 with $P_R = 35\%$, $P_{CH_4}/P_{H_2} = 1/4$, $\beta = 3$ K/min, $Q_{WO_3} = 94.3$ mg, $F = 50.5$ cc/min. (a) Partial pressure evolution of CH_4, H_2, H_2O, and CO according to temperature. (b) Mass balance calculation according to temperature of the amount of oxygen removed from the solid relative to tungsten (O/W) and of carbon retained by the solid (C/W).

The three figures illustrate the diversity of phenomena that may occur during the reduction and carburization of WO_3 by CH_4/H_2 mixtures.

Reactant pressures, in particular H_2, strongly affect the temperature of reduction, as already noticed (22), by shifting the reduction temperature to lower values with increasing pressures.

The reduction proceeds through two main steps with eventually a shoulder in the rising side of the first peak of reduction. It is generally admitted (20, 22) that this corresponds to the following sequence of steps:

$$WO_3(\rightarrow W_{20}O_{58}) \rightarrow WO_2 \rightarrow W. \qquad [1]$$

However, this sequence is observed only in the experiments with low reactant pressures ($P_R = 10$ or 35%), whereas with 90% of P_R, the residual O content after the first peak is significantly lower than 2 O/W (as low as 1.5 O/W). This trend can be found in all experiments (Tables 1 and 2) conducted in such a way as to lower the temperature of the first reduction peak (e.g., with higher pressure (Carb-C), with low heating rates (Carb-D), or low precursor loadings (Carb-J)).

This would suggest that the lower the temperature at which the overall reduction occurs, the higher the proportion of the first peak of reduction (e.g., compare Carb-D, -B, -E, and -F for an effect of β with the same reactants pressures and precursor loadings).

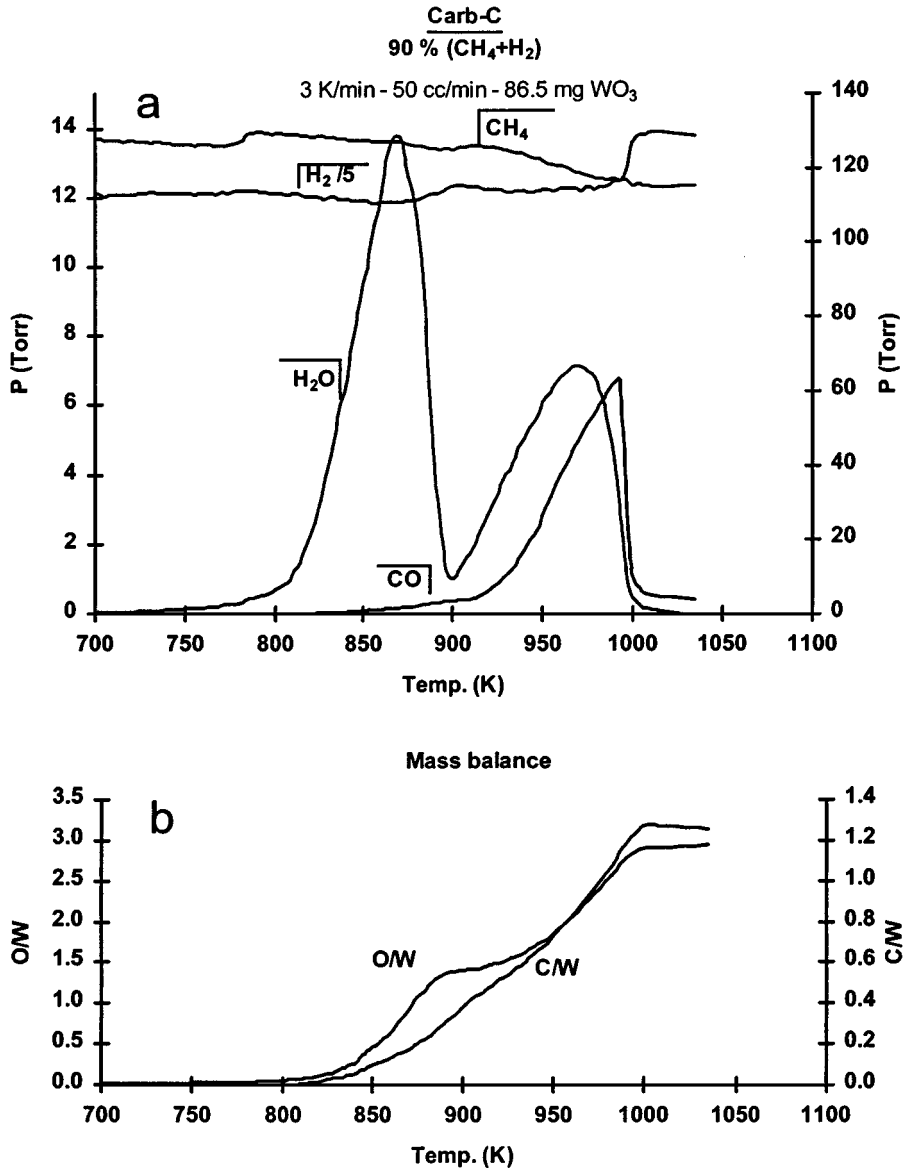

FIG. 3. Carb-C, temperature programmed reaction of WO_3 with $P_R = 90\%$, $P_{CH_4}/P_{H_2} = 1/4$, $\beta = 3$ K/min, $Q_{WO_3} = 86.5$ mg, $F = 50.0$ cc/min. (a) Partial pressure evolution of CH_4, H_2, H_2O, and CO according to temperature. (b) Mass balance calculation according to temperature of the amount of oxygen removed from the solid relative to tungsten (O/W) and of carbon retained by the solid (C/W).

The consumption of CH_4 also behaves very differently according to the pressure of reactants. In Carb-A (Fig. 1), CH_4 begins to react with the solid during the second peak of reduction and in a first stage only contributes to the reduction process by producing CO. When globally the O/W stoichiometry reaches 1 (maximum of the second peak of reduction), CH_4 brutally reacts to form slightly higher amounts of CO but mainly a carbide phase since most of the C is actually retained by the solid.

The carbon uptake actually occurs in two stages with an intermediary stoichiometry of approximately C/W = 0.5. The second C uptake occurs rapidly only after all the oxygen has been removed from the solid.

This suggests that, under these conditions, the carburization may proceed through a W_2C intermediate, whereas the total carburization to WC may occur only in the absence of O in the solid.

The behavior of Carb-C is very different as the carbon uptake occurs from the beginning of the reduction. Furthermore, little CO is formed in the earlier stage of reduction. CO production begins only at higher temperatures and contributes largely to the second stage of reduction. The evolution of the C/W stoichiometry does not show any marked passing through a composition corresponding to W_2C.

The case of Carb-B is intermediate, as the phenomena resemble those of Carb-A but at lower temperatures. Note,

however, that no clear transition through an intermediary composition near W_2C can be seen.

Compensating effects of reactant pressures, heating rate, and sample mass. Clearly different phenomena occur according to the experimental conditions. However, as far as the reduction process is concerned, similarities between TPR profiles are found for those sets of parameters that induce the reaction peak to occur in the same temperature range. For example, reduction with low reactant pressures and low heating rate (Carb-D: $P_R = 35\%$, $\beta = 1$ K/min) is similar to that of a higher pressure but also of a higher β experiment (Carb-C: $P_R = 90\%$, $\beta = 3$ K/min). Furthermore, these two experiments have similar patterns as Carb-J performed with intermediate values (Carb-J: $P_R = 35\%$, $\beta = 3$ K/min) but where the lower P_R, with respect to Carb-C, or higher β, with respect to Carb-D is compensated by a lower precursor loading of 25.2 mg of WO_3 instead of around 97 mg.

This suggests that the reduction process proceeds through different mechanisms according to the temperature range.

Sample mass effect on the reduction kinetics. Figure 4 shows the evolution of water pressure during the reduction–carburization with different loadings of WO_3. Methane and CO curves have been omitted for the sake of clarity as their contribution to the reduction process is minor and occurs only in the second peak of reduction.

The rate of reduction of these experiments may be compared in the rising part of each reduction peak. At 850 K, for example, one may compare the effect of the loading for the first reduction peak as, for all four experiments, this temperature corresponds to the rising part of the peak and one can therefore expect that the exhaustion of the oxygen in the solid would not significantly affect the kinetics of the reaction.

TABLE 3

Rate of H_2O Production in Carb-J, Carb-B, Carb-L, and Carb-K Measured at 850 K

Sample	Q_{WO_3} (mg)	Flow (cc/min)	P_{H_2} (Torr)	P_{H_2O} (Torr)	R_{H_2O} (μmol/min)	R_{H_2O}/P_{H_2} (μmol/min · Torr)
Carb-J	25.2	50.2	208	0.67	1.21	8.9×10^{-3}
Carb-B	94.3	50.5	219	1.09	3.02	1.38×10^{-2}
Carb-L	135	32.8	174	1.88	3.33	1.94×10^{-2}
Carb-K	266	50.5	214	2.95	8.19	3.83×10^{-2}

Table 3 summarizes the reaction rate measured at this temperature. Figure 5 shows the rate of H_2O formation as a function of WO_3 loading as well as the corrected rate assuming a first-order parameter for H_2.

It clearly appears that the reaction is first order toward the WO_3 loading also.

The behavior during the second peak is very different. Figure 4 shows that the water pressure is the same in the rising part of the three experiments whatever the amount of WO_3. This observation may eventually be extrapolated to the fourth experiment with the smaller loading. Of course, the maximum of water pressure is reached at higher

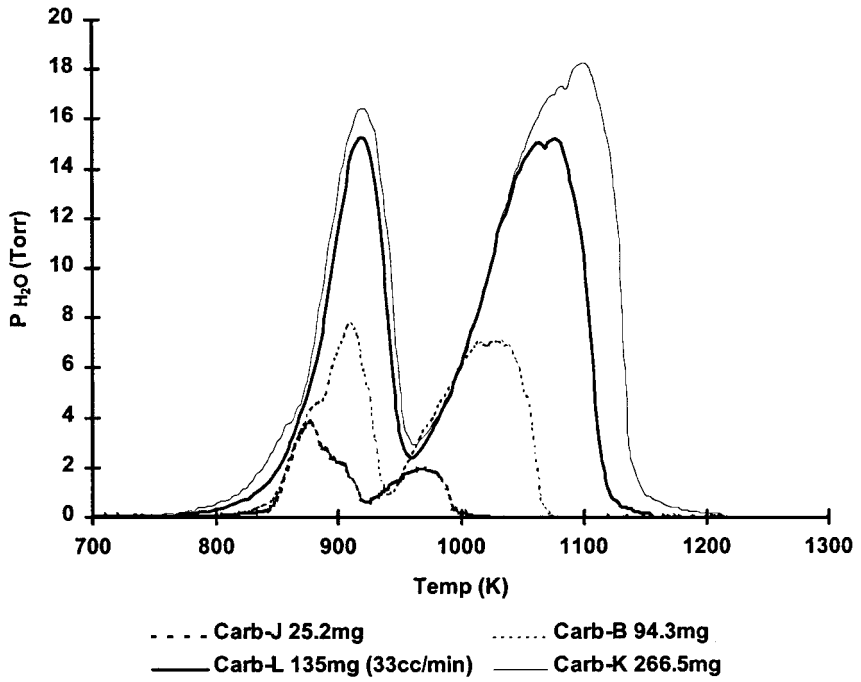

FIG. 4. Water pressure evolution in experiments Carb-J, Carb-B, Carb-L, and Carb-K with varying amounts of precursor (respectively $Q_{WO_3} = 25.2$, 94.3, 135, and 266.5 mg). Other experimental conditions are $P_R = 35\%$, $P_{CH_4}/P_{H_2} = 1/4$, $\beta = 3$ K/min, $F \sim 50$ cc/min (except for Carb-L, F = 33 cc/min).

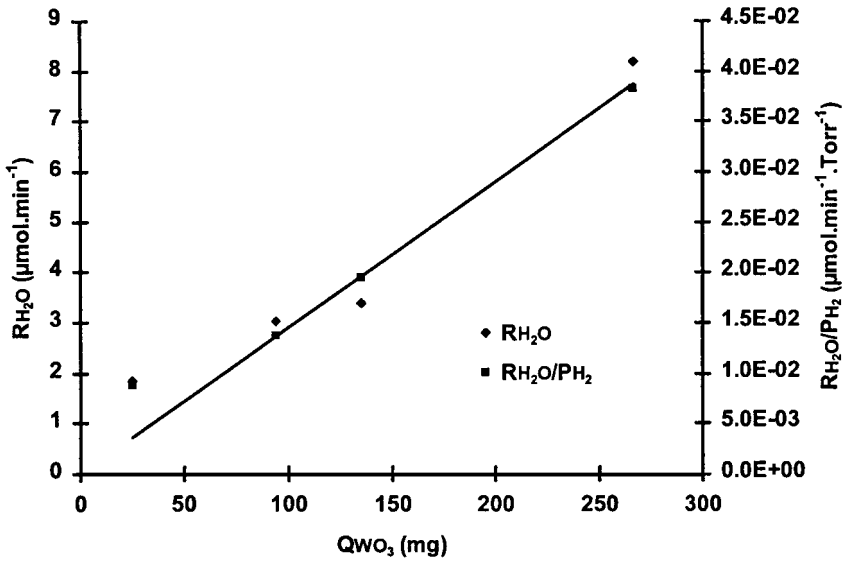

FIG. 5. (Left axis) Rate of H_2O formation acording to Precursor amount measured at 850 K. (Right axis) Rate corrected assuming first-order reaction according to H_2 pressure.

temperatures with increasing amounts of oxide due to the larger amount of O in the samples. It should be noted that it is not the reaction rate that is independent of the amount of solid but the actual water pressure as a different flow rate was used for one experiment (Carb-L).

This clearly suggests that the rate-determining step for the second peak of reduction is the removal of water from the reactor and that the solid is actually in equilibrium with the gas phase.

Considering that the maximum of the second peak of reduction is reached for a residual oxygen content of 1 O per W (O/W = 1), we may suppose that the reaction in equilibrium would be the following:

$$WO_2 + H_2 = WO + H_2O. \qquad [2]$$

Unfortunately, no thermodynamic data exist on such a WO phase, as it is certainly unstable.

This behavior during the second peak of reduction shows:

(i) that, above 900–950 K, the solid being in equilibrium, the diffusion rate of reduced species or of oxygen is high enough to allow the total uniformization of the composition within the solid particles;

(ii) that the space velocity is an important factor in the synthesis of carbide materials as already noticed (23) but the reason for this is not the lowering of the water pressure during the reduction but the lowering of the temperature at which the reduction terminates due to the exhaustion of the oxygen, the rate being dependent essentially on the flow rate.

Temperature Programmed Reactions: CH_4–D_2

Two experiments have been made using D_2 instead of H_2 in the carburizing mixture (Carb-P and Carb-O) using similar experimental conditions as for experiments Carb-M and Carb-A, respectively.

The aim of these experiments is to show possible interactions of methane with the solid, which would lead to exchange products, before CH_4 is actually consumed to produce CO or the carbide phase.

In practice only the products of monodeuteration (CP_3D) and perdeuteration (CD_4) are generally observed as initial products of reaction on metal catalysts (24, 25). Intermediate products (CP_2D_2 and CPD_3) are observed only at high conversion due to the dilution of D_2 by light hydrogen (noted as P, protium, whereas the symbol H is used when no distinction is made between P and D).

On tungsten metal, CP_3D is known to be the most abundant product (26). Due to the interference of water (P_2O, PDO, and D_2O), the experiments using D_2 cannot be analyzed quantitatively. They may, however, be compared to those using H_2 under the same experimental conditions.

Figures 6 and 7 show the evolution of a selected number of mass spectrometer signals in parallel to the quantitative analysis obtained using H_2 (bottom).

The following masses have been chosen from the D_2 experiments:

- $m/e = 15$ to represent mainly unreacted methane (CP_3^+)
- $m/e = 17$ for monodeuterated methane (CP_3D^+)
- $m/e = 20$ for D_2O^+ from the reduction (but also coincides with CD_4^+)
- $m/e = 3$ for HD^+ produced by the exchange reaction
- $m/e = 28$ for CO^+.

The reaction conditions were chosen to obtain a high temperature of reduction and carburization in one case (low

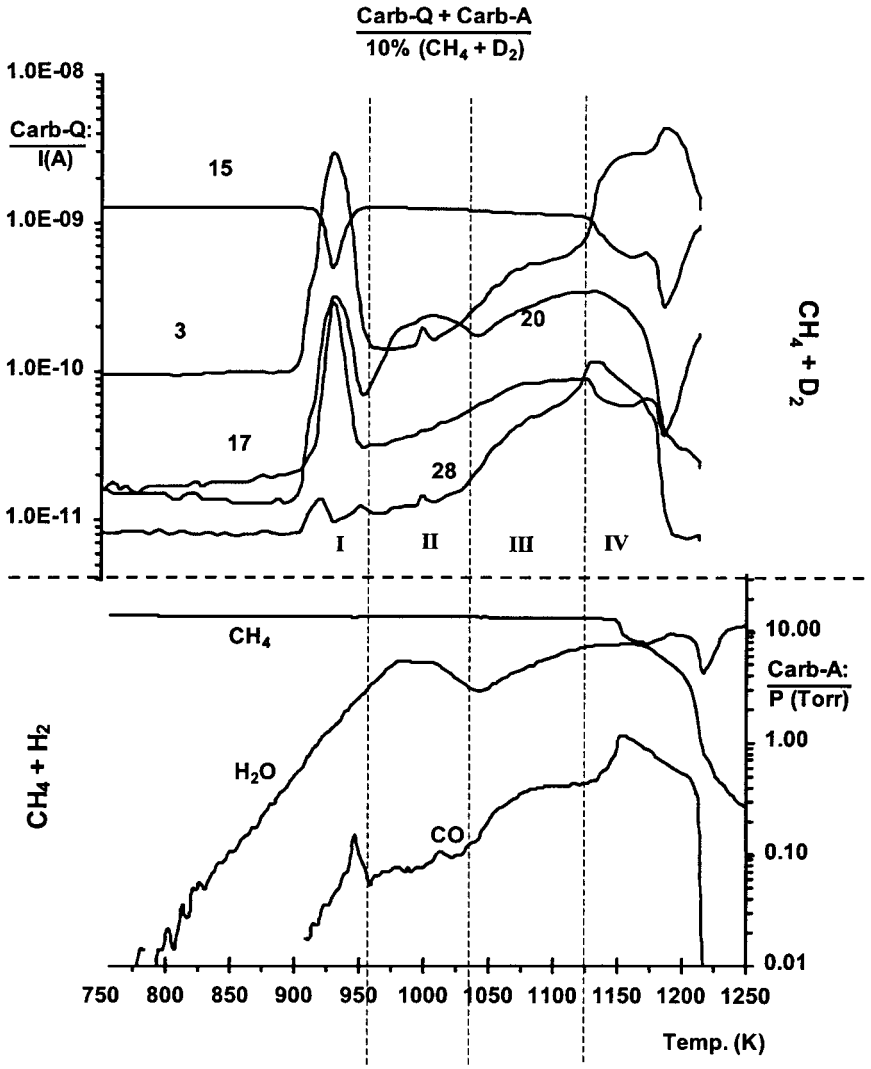

FIG. 6. Carb-Q, temperature programmed reaction of WO_3 using D_2 instead of H_2. (Top) Mass spectrometer signals for $m/e = 15$, 17, 20, and 28. (Bottom) Evolution of CH_4, H_2O, and CO partial pressures according to temperature in experiment Carb-A performed under similar experimental conditions with H_2 (see Table 1).

pressure of reactants) and a low temperature range in the other experiment (high pressure of reactants).

Low reactant pressure reaction (Fig. 6). The reaction with deuterium may be divided into four main parts (noted I to IV).

During the first part, an important consumption of light CH_4 occurs with the production of CP_3D and some CD_4 ($m/e = 20$), this latter summing up with the production of water due to the reduction.

Of course, the CH_4 consumption does not appear using H_2 but shows that in the rising part of the first reduction peak methane does actually interact with the surface. As this leads to only an extremely small production of CO it is reasonable to believe that this interaction is due to the presence of a metallic phase at the surface of the solid at this stage of the reduction.

The presence of a metallic phase, or of highly reduced tungsten species, at the surface of the solid being reduced is not a surprise. What is more striking, however, is that the exchange reaction stops brutally when the temperature increases (Part II).

As thermodynamically and kinetically there is no reason why the reaction should stop at increasing temperatures the only plausible explanation is that the catalytically active species actually disappear by the diffusion of the metal into the bulk of the solid (or of oxygen toward the surface).

This phenomenon must occur sufficiently rapidly that the mean residence time of the reduced species at the surface is so small as to totally forbid any exchange reaction to occur.

The second part of the TPR corresponds to the completion of the first reduction peak as observed using H_2. Only small amounts of deuterated methane are observed during this period.

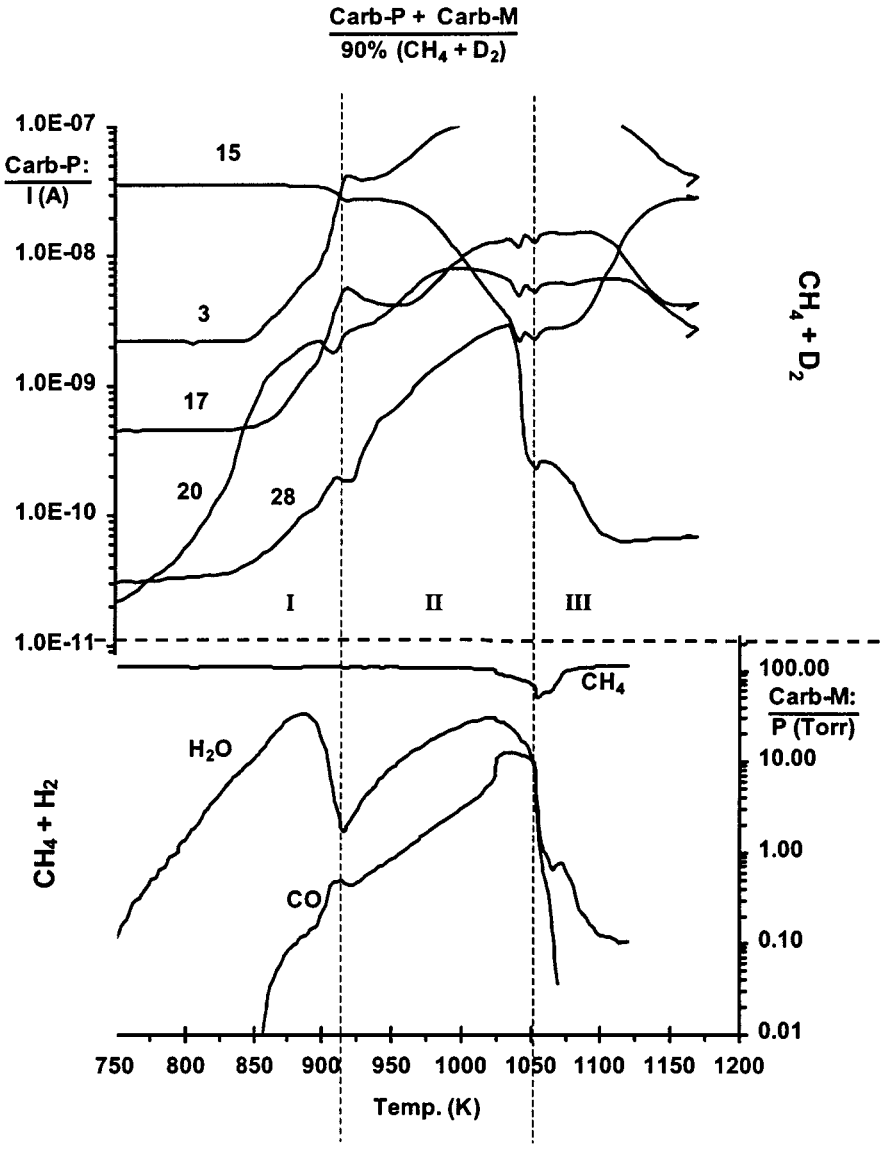

FIG. 7. Carb-P, temperature programmed reaction of WO_3 using D_2 instead of H_2. (Top) Mass spectrometer signals for $m/e = 15$, 17, 20, and 28. (Bottom) Evolution of CH_4, H_2O, and CO partial pressures according to temperature in experiment Carb-M performed under similar experimental conditions with H_2 (see Table 1).

In the third part (first half of the second reduction peak), small amounts of CH_4 are consumed to produce some CP_3D and CO.

Finally, in the last part, methane is consumed again, but to produce mainly the carbide and some CO. When the reduction and carburization is terminated, the production of CP_3D increases significantly due to the catalytic activity of tungsten carbide.

High reactant pressure reaction (Fig. 7). In this experiment, only three stages can be observed.

The first, corresponding to the first reduction peak, is accompanied by an increasing production of exchange products (HD, CP_3D, and eventually CD_4). The consumption of light methane by exchange is difficult to observe on the graph due to the high CH_4 pressure as compared to the previous experiment.

In the second stage of the reaction, corresponding to the second reduction peak, the exchange slightly slows down to increase again at the end of the reduction.

During the carburization, high amounts of deuterated methane continue to be observed. However, the activity slows down when the solid is fully carburized, probably due to the deposition of amorphous carbon at the surface of the catalysts.

We thus see that on the contrary to the other experiment with D_2, at higher reactant pressure and consecutively lower temperatures of reduction, the exchange reaction occurs all over the reduction process.

TABLE 4

Rate of CH_4 Consumption at 925 K in Carb-Q and Carb-P

Sample	P_R (%)	Q_{WO_3} (mg)	P_{D_2} (Torr)	P_{CH_4} (Torr)	Conv. (%)	R_{CP_3D} (μmol min^{-1} mg^{-1})
Carb-Q	10	108.9	61	15	53	0.20
Carb-P	90	277	540	147	23	0.34

This is not surprising as it has already been mentioned that at high pressure, carbon from CH_4 begins to be retained by the solid very early in the reduction process, contrary to what happens at low reactant pressure (and thus high reaction temperature).

Another interesting information may be obtained by comparing the actual rates of the exchange reaction at a same temperature for both experiments.

Table 4 shows the reaction rates measured at 925 K for both experiments. This temperature corresponds to the maximum rate observed at low reactant pressure in the first stage of reduction while remaining in the rising part of the exchange activity of the peak observed in the high reactant pressure experiment.

The reaction rates have been estimated by measuring the conversion of light methane ($m/e=15$). This table shows that although the reactant pressure is 9 times higher in Carb-P the actual rate of exchange is only 1.7 times higher than that in Carb-Q.

This can be expressed by writing the formal reaction rate equation,

$$R = k \cdot p_{D_2}^{\alpha} \cdot p_{CH_4}^{\beta}, \qquad [3]$$

and considering a unitary order with respect to methane ($\beta=1$). The rates shown in Table 4 allow the calculation of the order with respect to D_2, giving a negative value of $\alpha=-0.8$.

This inhibiting effect may be explained by the effect of hydrogen pressure on the rate of CH_4 adsorption at the surface of the solid. An associative mechanism has been proposed for this adsorption step (26, 27) taking into account the ensemble effect which considers that the adsorbed radical needs more than one active site:

$$CH_4 + H_{ads} + zS \Leftrightarrow CH_{3\ ads} + H_2 + wS. \qquad [4]$$

For such a mechanism, in the case of methane–deuterium exchange the H_{ads} is essentially deuterium and therefore all the methane molecules which react will produce exchange products. The total rate of exchange is therefore equal to the rate of adsorption (28), which may be expressed as

$$R = R_a = k \cdot p_{CH_4} \cdot \theta_H \cdot \theta_S^z. \qquad [5]$$

Assuming that θ_c is negligible,

$$\theta_S = 1 - \theta_H - \theta_C \approx 1 - \theta_H, \qquad [6]$$

Eq. [5] becomes

$$R_a = k \cdot p_{CH_4} \cdot \theta_H \cdot (1-\theta_H)^z = k \cdot p_{CH_4} \cdot G_R, \qquad [7]$$

with

$$G_R = \theta_H \cdot (1-\theta_H)^z. \qquad [8]$$

The H_2 pressure, or D_2 in this case, will influence the reaction rate through the intermediate of the H coverage. Assuming that the active surface is essentially tungsten metal, the H coverage may be evaluated approximately considering an adsorption enthalpy of 125 kJ/mol (29) and an entropy of 130 J/mol · K, values which are usual for metallic catalysts (30).

From

$$\theta_H = \frac{\sqrt{K \cdot p_{H_2}}}{1+\sqrt{K \cdot p_{H_2}}}, \qquad [9]$$

where K is the adsorption equilibrium constant and

$$K = e^{-\frac{\Delta G_{ads}}{RT}}, \qquad [10]$$

we may calculate the H coverage at 925 K for both experiments and, assuming a value of $z=6$ (31), the corresponding values of G_R which are reported in Table 5.

This table shows that the inhibiting effect of hydrogen on the interaction of methane with the surface of the material is considerable and that the higher rates observed with 90% of reactants is due only to the compensating effect of the simultaneous increase of the CH_4 pressure.

The existence of such an important inhibiting effect of H_2 on the interaction of CH_4 with the solid has serious consequences as it means that it is not possible to optimize the reduction process (e.g., by increasing the H_2 pressure) independently from consequences on the carburization process while such a possibility was claimed in the past (10).

Temperature-Programmed Reaction: In Situ XRD Study

Three *in situ* experiments were made using different reactant pressures, respectively 10, 30, and 100% of atmospheric pressure, and a CH_4/H_2 ratio of 1/4. Other parameters were kept constant, such as the heating rate of 1.2 K/min. The temperature ramp had, however, to be interrupted for about 10 min at different temperatures to allow

TABLE 5

G_R Values Calculated for Carb-Q and Carb-P at 925 K

Sample	P_{D_2} (Torr)	θ_H	G_R	$G_R \cdot P_{CH_4}$
Carb-Q	61	0.24	4.6×10^{-2}	0.69
Carb-P	540	0.50	8.1×10^{-3}	1.19

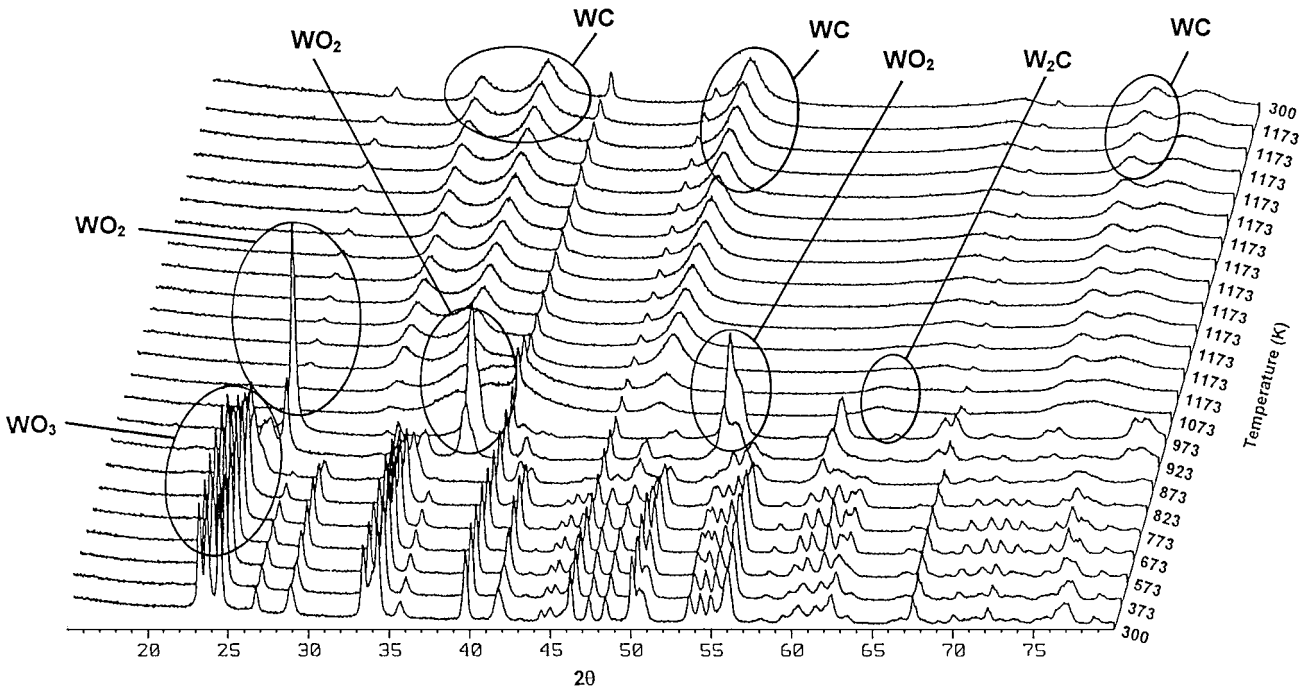

FIG. 8. X-ray diffraction patterns at different temperatures during *in situ* temperature programmed reaction of WO_3 ($P_R = 10\%$).

the measurement of the diffraction diagram. Due to this particularity it is difficult to compare directly the XRD results with those obtained by the TPR experiments following the gas phase composition.

Interesting information may nevertheless be found by comparing these three experiments with each other.

Figures 8, 9, and 10 show the diffraction diagrams obtained at different temperatures for these samples. The diffraction peaks of the most interesting compounds have been emphasized on the diagrams.

Table 6 summarizes the most abundant species observed at some temperatures for the three experiments.

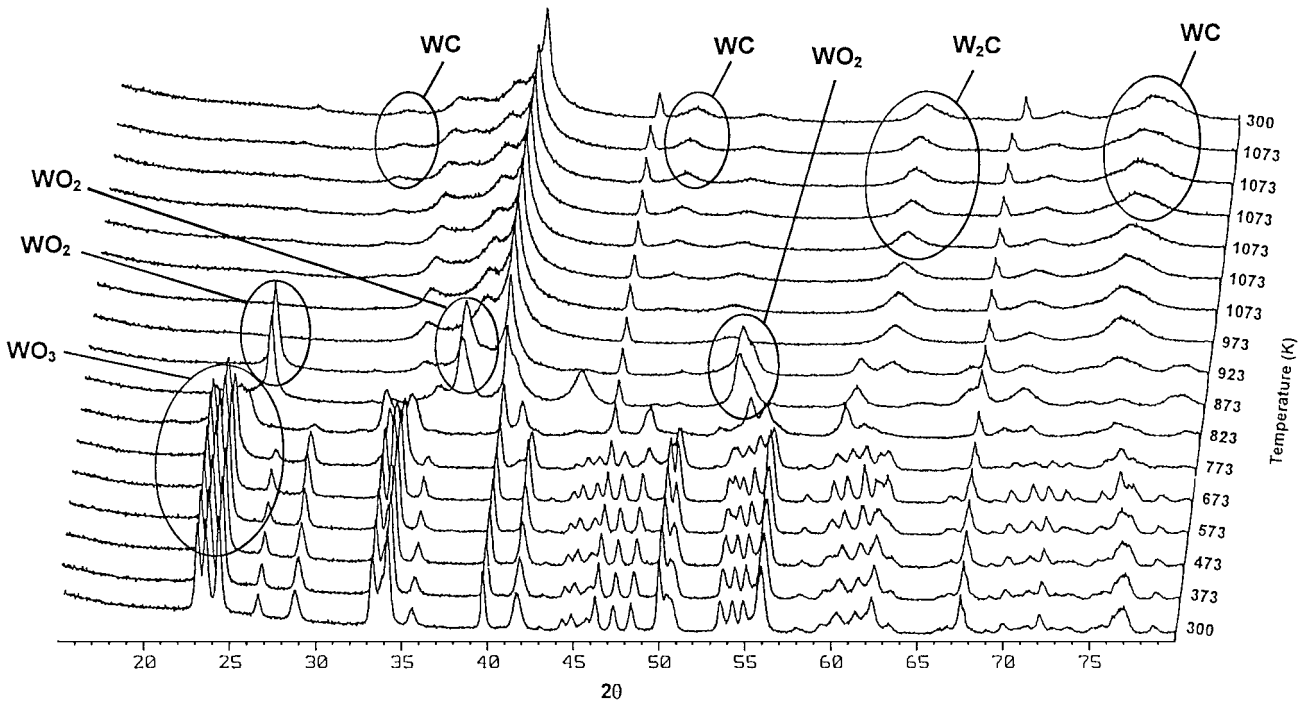

FIG. 9. X-ray diffraction patterns at different temperatures during *in situ* temperature programmed reaction of WO_3 ($P_R = 30\%$).

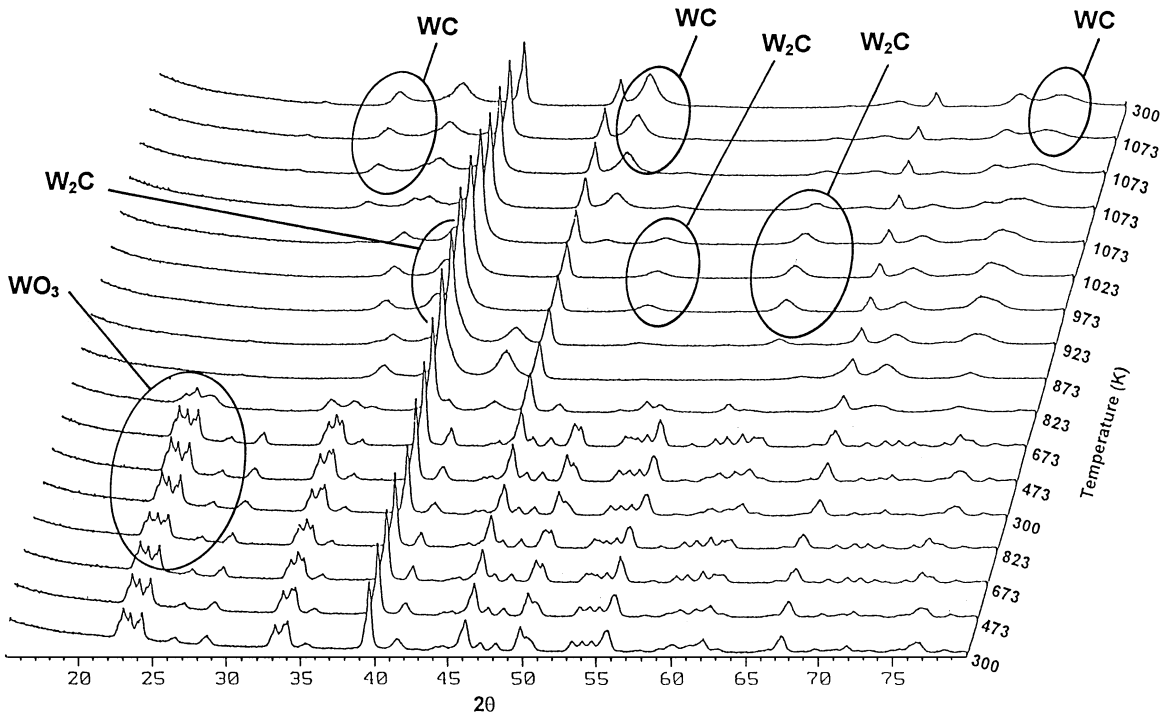

FIG. 10. X-ray diffraction patterns at different temperatures during *in situ* temperature programmed reaction of WO_3 ($P_R = 100\%$).

It is seen from this table that, as it should be expected the reduced phases appear at lower temperatures as the reactant pressures increase. The most interesting information, however, is that the lower the pressure is, the more defined the intermediate steps are.

For example, under the lowest-pressure reaction the following steps are clearly defined:

$$WO_3 \rightarrow W_{20}O_{58} \rightarrow WO_2 \rightarrow W_2C \rightarrow WC, \qquad [11]$$

whereas under the higher-pressure conditions the WO_2 phase does not appear at all.

TABLE 6

Most Abundant Crystallographic Phases Observed at Different Temperatures during *In Situ* Temperature Programmed Reaction of WO_3 with CH_4 and H_2 at $P_R = 10$, 30, and 100% of Atmospheric Pressure

T(K)	P_R, 10%	P_R, 30%	P_R, 100%
823	WO_3	$W_{20}O_{58}-W_{2.9}$	$W_{20}O_{58} + W_3$(C/O)
873	$WO_3 + W_{20}O_{58}$	$WO_2 + W_3$(C/O)	W_3(C/O)
923	$WO_2 + W_{20}O_{58}$	$WO_2 + W_2C + (W_3$(C/O))	W_2C ($+W_6C_{2.54}$)
973	WO_2	W_2C	W_2C
1023			W_2C
1073	$W_2C + WC$	$W_2C + WC$	WC ($+W_2C \searrow$)
1173	$WC + W_2C$		
1173	WC		

However, a highly reduced specie W_3O (or even slightly carburized W_3C) appears at low temperature and this in the presence of an oxide phase.

GENERAL DISCUSSION

According to the reaction conditions, the reduction and carburization of WO_3 may occur in a wide range of temperatures. Two distinct behaviors have been observed on both the reduction and the carburization processes according to the temperature.

Low-temperature reactions are induced by higher reactant pressures, lower heating rates, and/or higher space velocities. In such conditions, the reduction and carburization occurs simultaneously in accordance with the fact that methane exchange occurs all along the reduction process. Furthermore, except for $W_{20}O_{58}$, no defined partially reduced phase such as WO_2 can be observed, again in accordance with the mass balance calculations which show that far more than 1 oxygen atom per W is extracted from the solid during the first reduction peak.

This suggests that under these conditions the reduction of the solid is not uniform but is accompanied by the formation of a highly reduced surface and a core of oxide. The surface is therefore able to interact with methane to produce exchange products with deuterium and eventually to carburize. This behavior is most clearly observed in the first reduction peak of the experiments at high reactant partial pressures. The rate-limiting step of this reduction process

is therefore the diffusion of the reduced W or of oxygen in the bulk of the particles.

During the second peak of reduction and in the whole reduction process for the low-pressure experiments the situation is very different. We have seen that during the second peak the solid is in equilibrium with the gas phase composition, meaning that the diffusion rate in the solid is no longer the rate limiting step but is replaced by the mass transport in the gas phase. This is also seen in the CH_4–D_2 experiment at low pressure where a peak of exchange occurs which clearly shows the disappearance of reduced species from the surface of the solid above 923 K. This temperature value can therefore be considered as a key value above which the diffusion phenomena in the solid can be considered as rapid as compared to gas–surface interactions and mass transport in the gas phase.

The following scheme can therefore be proposed for the reduction–carburization of WO_3 by CH_4/H_2 mixtures. If the reduction begins at temperatures below ~900 K (for example due to high H_2 pressure) a metallic phase is produced at the surface of the solid, leading to the simultaneous activation of methane which may participate in the reduction process or eventually carburize the solid although its bulk is still highly oxidized (WO_3 or $W_{20}O_{58}$).

Under these conditions the diffusion rate within the solid is the rate-limiting step of the overall process. When the temperature reaches around 900 K, the diffusion rate increases rapidly, generating a second reduction peak during which some of the oxygen reacts with the carbon already retained by the solid to produce the relatively large amount of CO observed in the high-pressure experiments.

When the reduction begins at temperatures higher than 900 K (e.g., due to low H_2 pressure), the entire process occurs while the diffusion rate in the solid is rapid with the eventual exception of the very beginning of the reduction. Under these conditions very well defined intermediates can be observed both by mass balance calculations and by *in situ* XRD experiments. The internal diffusion within the particles being rapid, the surface is continuously replenished in oxygen and is thus unable to activate CH_4 (neither for exchange with D_2 nor for the reduction–carburization) and the carburization begins only when the solid is reduced to an overall stoichiometry lower than WO_1.

In most cases, the carburization is limited to W_2C when oxygen is still present in the solid, whereas WC is formed only after total reduction.

CONCLUSIONS

This work shows that two mechanisms exist for the reduction–carburization of powder WO_3 by CH_4/H_2 mixtures for the synthesis of WC catalysts. These two mechanisms occur according to the temperature range which itself is affected by several experimental parameters. The most important one is certainly the partial pressure of the reactants (CH_4 and H_2) but may be emphasized or compensated by the heating rate and the space velocity.

A key temperature range of 900–923 K has been defined above which the diffusion rate within the solid is no longer a limiting step for the reduction–carburization process.

One should therefore keep in mind that the lowering of the synthesis temperature—for example in order to avoid the sintering of the catalyst and the loss of specific surface area—may lead to nonuniform materials. On the contrary, in order to determine the intrinsic properties of such material in catalysis one should pay close attention in obtaining well defined and uniform materials even at the expense of specific surface area.

Furthermore, it has also been shown that the main effect of increasing the space velocity is to lower the temperature of the end of reduction, whereas, at a given temperature, the water pressure is unaffected by the space velocity as long as the solid still contains significant amounts of oxygen.

Finally, our work has highlighted the strong inhibiting effect of H_2 on the interaction of the solid with methane. As a consequence, one cannot independently optimize the reduction process by H_2 without strongly affecting the carburization by CH_4.

ACKNOWLEDGMENTS

This work was supported by a stimulation Contract ST2J-0467-C(TT) from the European Commission. One of the authors (A.L.) wishes to express his gratitude toward the David and Alice Van Buuren Foundation for his research grant.

REFERENCES

1. Oyama, S. T., *Catal. Today* **15**, 179 (1992).
2. Leclercq, L., Prigent, M., Daubrege, F., Gengembre, L., and Leclercq, G., *in* "Catalysis and Automotive Pollution Control (CAPoC)" (A. Crucq and A. Frennet, Eds.), Vol. 30, p. 417. Elsevier, Amsterdam, 1987.
3. Bronoel, G., Museux, E., Leclercq, G., Leclercq, L., and Tassin, N., *Electrochim. Acta* **36**, 1543 (1991).
4. Guskey, G. J., Boudart, M., and Frennet, A., *in* "Hydrogen Behaviour and Mitigation in Water-cooled Nuclear Power Reactors" (E. Della Loggia, Ed.), p. 398. Commission des Communautés européennes, Luxembourg, 1992.
5. Boudart, M., Oyama, S. T., and Leclercq, L., *in* "Proceedings 7th International Congress on Catalysis" (T. Seiyama and K. Tanake, Eds.), p. 578. Elsevier, Amsterdam, 1981.
6. Saito, M., and Anderson, R. B., *J. Catal.* **63**, 438 (1980).
7. Djéga-Mariadassou, G., Boudart, M., Bugli, G., and Sayag, C., *Catal. Lett.* **31**, 411 (1995).
8. Markel, E. J., and Van Zee, J. W., *J. Catal.* **126**, 643 (1990).
9. Keller, V., Wehrer, P., Garin, F., Ducros, R., and Maire, G., *J. Catal.* **153**, 9 (1995).
10. Iglesia, E., Ribeiro, F. H., Baumgartner, J., and Boudart, M., *Catal. Today* **15**, 307 (1992).
11. Frennet, A., *et al.*, *in* "Proceedings, 10th International Congress on Catalysis, Budapest, 1992" (L. Guczi, F. Solymosi, and P. Tétényi, Eds.), p. 927. Akadémiai Kiado, Budapest, 1993.

12. Levy, R. B., and Boudart, M., *Science* **181**, 547 (1973).
13. Rodrigues, J. A. J., Cruz, G. M., Bugli, G., Boudart, M., and Djéga-Mariadassou, G., *Catal. Lett.* **45**, 1 (1997).
14. Boudart, M., Oyama, S. T., and Volpe, L., U.S. patent 4,515,763 (1982).
15. Volpe, L., and Boudart, M., *J. Solid State Chem*. **59**, 348 (1985).
16. Lee, J. S., Volpe, L., Ribeiro, F. H., and Boudart, M., *J. Catal.* **112**, 44 (1988).
17. Volpe, L., and Boudart, M., *Catal. Rev. Sci. Eng.* **27**, 515 (1985).
18. Volpe, L., Oyama, S. T., and Boudart, M., *in* "Preparation of Catalysts III" (G. Poncelet, P. Grange, and P. A. Jacobs, Eds.), p. 147, Elsevier, Amsterdam, 1983.
19. Löfberg, A., Seyfried, L., Blehen, P., Decker, S., Bastin, J. M., and Frennet, A., *Catal. Lett.* **33**, 165 (1995).
20. Leclercq, G., Kamal, M., Giraudon, J. M., Devassine, P., Feigenbaum, L., Leclercq, L., Frennet, A., Bastin, J. M., Löfberg, A., Decker, S., and Dufour, M., *J. Catal.* **158**, 142 (1996).
21. Giraudon, J. M., Leclercq, L., Leclercq, G., Löfberg, A., and Frennet, A., *J. Mater. Sci.* **28**, 2449 (1993).
22. Vermaire, D. C., and van Berge, P. C., *J. Catal.* **116**, 309 (1989).
23. Oyama, S. T., Schlatter, J. C., Metcalfe III, J. E., Lambert, J. M., Jr., *Ind. Eng. Chem. Res.* **27**, 1639 (1988).
24. Kemball, C., *Advan. Catal.* **11**, 223 (1959).
25. Frennet, A., and Liénard, G., *Surf. Sci.* **18**, 80 (1969).
26. Frennet, A., *Catal. Rev. Sci. Eng.* **10**, 37 (1974).
27. Frennet, A., *Catal. Today* **12**, 131 (1992).
28. Frennet, A., *in* "Elementary Reation Steps in Heterogeneous Catalysis" (R. W. Joyner and R. A. van Santen, Eds.), NATO ASI Series C398. Kluwer Academic, Dordrecht, 1993.
29. Trapnell, B. M., *in* "Chemisorption," p. 127. Academic Press, London, 1955.
30. Crucq, A., Degols, L., Liénard, G., and Frennet, A., *Acta Chim. Acad. Sci. Hung.* **111**, 547 (1982).
31. Martin, G. A., *Bull. Soc. Chim. Belg.* **105**, 131 (1996).